that was measured at $I/I_{SAT} = 1$ and are plotted as a function of I/I_{SAT} in Figure 10. Figure 10 shows that the maximum reflectivity, hence signal-to-noise ratio, is obtained at intensities approximately equal to I_{SAT}. The highest signal-to-noise ratios also were observed experimentally at these intensities. As the laser intensity increases above I_{SAT}, the line-center signal intensity becomes constant, the peak profiles power broaden, and the scattered-light-noise-baseline increases. The combined result is that the signal-to-noise ratio decreases. Working at powers much greater than I_{SAT} will not improve the detection limit of DFWM, but will only diminish the advantages of the technique, such as narrow sub-Doppler line shapes.

VI. Conclusions

In this paper we report the first DFWM study of the CH radical and have demonstrated that trace flame species can be detected at atmospheric pressure with high sensitivity using DFWM. Accurate CH concentration profiles and vibrational temperatures with regard to LIF results have been obtained without having to make corrections for collisional processes. At atmospheric pressure the DFWM and LIF intensities are comparable; however, at higher pressures DFWM should prove to be more sensitive than LIF because of the effect of quenching collisions on the LIF signal. An additional advantage of DFWM is that it generates a coherent signal beam that can be remotely detected with high efficiency. This attribute enables nonintrusive investigation of many important chemical environments that suffer from limited optical access, high levels of emitted radiation, and high pressures, such as plasmas, flashes, flames, and discharges. DFWM will be especially advantageous for the detection of molecular species that do not fluoresce or whose fluorescence is complicated by collisional effects.

Acknowledgment. We are grateful to L. A. Rahn, R. L. Farrow, D. J. Rakestraw, and M. A. Cappelli for helpful discussions. Skip Williams thanks the Air Force Office of Scientific Research for a U.S. Air Force Laboratory Graduate Fellowship, and David S. Green acknowledges the Natural Sciences and Engineering Research Council of Canada for a postdoctoral fellowship. This work was supported by the Air Force Office of Scientific Research (AFOSR-F4962-92-J-0074).

Registry No. CH radical, 3315-37-5.

Isomers and Reactivity of C_3N^+: An Experimental Study

Simon Petrie,[†] Kathryn M. McGrath,[‡] Colin G. Freeman, and Murray J. McEwan*

Contribution from the Department of Chemistry, University of Canterbury, Christchurch, New Zealand. *Received December 27, 1991. Revised Manuscript Received April 17, 1992*

Abstract: The C_3N^+ ion, generated by electron impact on HC_3N and C_4N_2 and as a product in several ion–molecule reactions, was found to exist in two isomeric forms: $CCCN^+$ and cylic C_3N^+. These forms were distinguished by their different reactivities with a range of neutral reagents in a selected-ion flow tube (SIFT). Isomeric identification was made by reference to existing ab initio calculations. The most reactive isomer, $CCCN^+$, was the major form (≥90%) of the C_3N^+ ion from all sources of production examined and was found to undergo collision-rate reactions with most of the neutral molecules studied. c-C_3N^+ was much less reactive, which implies an activation barrier in its reactions as it is the higher energy form. Product distributions are reported for the reactions of $CCCN^+$, and rate coefficients for the reactions of both isomers with H_2, CH_4, NH_3, H_2O, N_2, O_2, CO, C_2H_2, HCN, CO_2, and C_2N_2 at 300 ± 5 K are also given.

Introduction

The circumstellar envelope of the star IRC+10216 is noted for containing a variety of interesting molecules that have been observed by radioastronomy techniques. Among the molecules detected was the first observation of the cyanoethynyl radical, CCCN,[1] which was identified from its calculated rotational spectrum.[2] Subsequently CCCN was observed within the cold interstellar cloud TMC-1.[3] Its isomer, the isocyanoethynyl radical CCNC, has also been proposed as an interstellar species[4] but has not yet been detected. A likely mechanism for the formation of C_3N in the interstellar environment is through dissociative recombination of protonated cyanoacetylene and similar ions and by photodissociation of HC_3N. The molecular ion of C_3N, C_3N^+, can also be produced in the interstellar medium and in planetary atmospheres when cyanoacetylene and associated nitriles are exposed to ionizing radiation, and it is this ion that forms the subject of the present study.

Electron impact is a commonly-used means of ionization in the laboratory, and the ion at $m/z = 50$, corresponding to C_3N^+, is a prominent component in the mass spectra of the nitriles HC_3N and NC_4N.[5-7] The value for $\Delta H_f°(C_3N^+) = 1929$ kJ mol^{-1} was first estimated from the appearance potentials for C_3N^+ generated from HC_3N and C_4N_2.[5] Subsequent experiments using the technique of monochromatic electron impact ionization lowered $\Delta H_f°(C_3N^+)$ to 1850 kJ mol^{-1} and also showed a sharp break in the ionization efficiency curve for C_3N^+ generated from HC_3N, 0.9 eV above the threshold for C_3N^+ production.[6] This break was interpreted as corresponding to the onset of formation of a higher energy species of C_3N^+: either a metastable excited ion or a structural isomer of the lower energy form. An ab initio investigation of the potential energy surface of C_3N^+ identified the lowest energy species as $CCCN^+$ and supported the break in the ionization efficiency curve as corresponding to the formation of a cyclic isomer with $\Delta H_f°(CCCN^+) = 1850$ kJ mol^{-1} and

[†] Present address: Department of Chemistry, York University, North York, Ontario, Canada M3J 1P3.

[‡] Present address: Department of Applied Mathematics (Physical Chemistry), Research School of Physical Sciences and Engineering, Australia National University, Canberra, ACT 2016, Australia.

(1) Guélin, M.; Thaddeus, P. *Astrophys. J.* **1977**, *212*, L81.
(2) Wilson, S.; Green, S. *Astrophys. J.* **1977**, *212*, L87.
(3) Friberg, P.; Hjalmarsson, Å.; Irvine, W. M.; Guélin, M. *Astrophys. J.* **1980**, *241*, L99.
(4) Stewart, G. W.; Henis, J. M. S.; Gaspar, P. P. *J. Chem. Phys.* **1972**, *57*, 1990.
(5) Dibeler, V. H.; Reese, R. M.; Franklin, J. L. *J. Am. Chem. Soc.* **1961**, *83*, 1813.
(6) Harland, P. W. *Int. J. Mass Spectrom. Ion Processes* **1986**, *70*, 231.
(7) Harland, P. W.; Maclagan, R. G. A. R. *J. Chem. Soc., Faraday Trans. 2* **1987**, *83*, 2133.

0002-7863/92/1514-9130$03.00/0

$\Delta H_f°(c\text{-}C_3N^+)$ = 1935 kJ mol^{-1}: a difference in $\Delta H_f°$ of 0.88 eV.[7] Also, a third isomeric structure, CCNC$^+$, was calculated to have an energy of formation in between these two values ($\Delta H_f°(CCNC^+) > \Delta H_f°(CCCN^+)$ by ~15 kJ mol^{-1}), but no experimental evidence was found to support its formation in the electron impact study.[6]

Preliminary studies in our laboratory of the reaction chemistry of C_3N^+ had earlier shown a difference in reactivity of C_3N^+[8] ions: one form being reactive with H_2 and CH_4 and the other form unreactive.[9] We have previously used the flow tube technique to distinguish between isomers on the basis of reactivity in several systems of nitriles including CH_3CNH^+/CH_3NCH^+,[10] CCN^+/CNC^+,[11] and HCN^+/HNC^+.[12] The CCN^+/CNC^+ system has also been investigated elsewhere using a similar technique.[13] We present here the results of a more extensive study into the chemistry of, and the distinction between, the two isomers of C_3N^+.

We also note that several studies of cations related to C_3N^+ have appeared in the literature with particular emphasis on the carbene character of the cation. As noted earlier, the lowest energy isomer of C_3N^+ is CCCN$^+$ which may be represented in its carbene form as :C=C=C=N:$^+$. Reactions of :CCCN$^+$ might therefore be expected to exhibit the characteristic behavior of carbenes such as coordination with a lone pair, insertion into σ-bonds, and addition to multiple bonds. Bohme et al. have examined the reactions of similar cations including :CCN$^+$[13] and :CCCCN$^+$[14] and have rationalized much of the chemistry of these ions in terms of their carbene character. Parent investigated reactions of :C_nN^+ (n = 4–8) with CH_4[15,16] while Parent and McElvany examined the reactions of the same :C_nN^+ series with HCN.[17] In both cases the ensuing chemistry is discussed in terms of initial carbene attack on the C–H bond of CH_4 or HCN.

Experimental Section

The present results were obtained using a selected-ion flow tube (SIFT) apparatus which has been described previously.[18] Measurements were obtained at room temperature, 300 ± 5 K, using a helium buffer gas at a pressure of 0.3 Torr. Neutral reagents were obtained commercially as high-purity reagents (99.5 mol % or better) and were further purified by vacuum distillation. HC_3N was synthesized from ammonolysis of methyl propiolate followed by dehydration of propynamide;[19] dicyanoacetylene, C_4N_2, was prepared by the action of ammonium hydroxide on dimethyl acetylenedicarboxylate followed by heating in calcined sand;[20] methylcyanoacetylene, CH_3C_3N, was prepared by the successive action of aqueous ammonia and P_2O_5 on methyl-2-butynoate.[21]

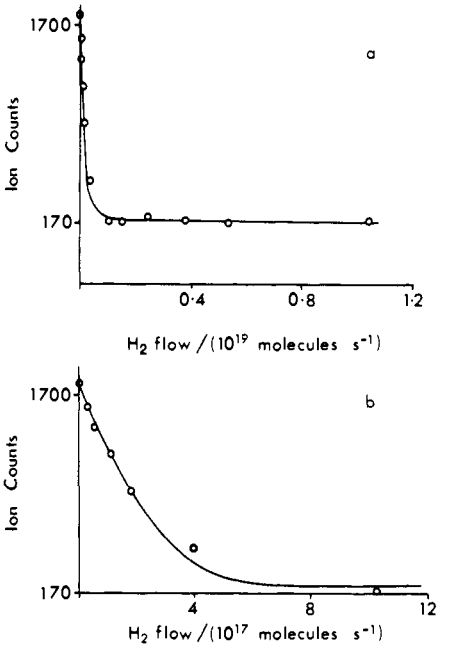

Figure 1. Observed semilogarithmic decay curve for the reaction of C_3N^+ (generated from electron impact on HC_3N) with H_2. (a) Graph showing the decay of the m/z = 50 signal over the entire range of H_2 flows covered. (b) Graph highlighting the initial rapid decay of the more reactive isomer. The points are experimental, and the curve is the computer-generated fit corresponding to a rate coefficient of $k \sim 1.0 \times 10^{-9}$ cm^3 s^{-1} for the reactive isomer and no reaction for the less reactive isomer.

All cyanoacetylenes and their derivatives were subsequently purified by several freeze–pump–thaw cycles under vacuum.

Experimental Results

Initially we produced C_3N^+ by electron impact (typically with 30-eV electrons) on HC_3N, in the ion source of the SIFT instrument. We confirmed that two different species of C_3N^+ were present in the m/z = 50 ion swarm from their subsequent reactions with H_2 and CH_4 which were introduced at the second inlet port of the flow tube. The more reactive component accounted for ~90% of the m/z = 50 signal and exhibited a near-collision-rate reaction with H_2 and CH_4 ($k_{H_2} = 8.1 \times 10^{-10}$ cm^3 s^{-1}; $k_{CH_4} = 9.7 \times 10^{-10}$ cm^3 s^{-1}). The other component displayed no detectable reactivity with either H_2 or CH_4, establishing an upper limit for $k < 1 \times 10^{-12}$ cm^3 s^{-1} for reactions between this component and these neutrals. The results for H_2 are summarized in Figure 1.

The choice of HC_3N as the ion source gas for C_3N^+ suffered from the disadvantage of an accompanying injection into the flow tube of the parent ion HC_3N^+, as an impurity which made product identification difficult. Alternative sources of the C_3N^+ ion were examined to see whether a cleaner source could be found and to see how the ratio of reactive to unreactive component changed with the parent molecule. Methylcyanoacetylene on electron impact gave fragment ions corresponding to C_4H^+ (m/z = 49) and HC_3N^+ (m/z = 51) as well as C_3N^+ (m/z = 50). The possibility of contamination of the m/z = 50 signal by $C_4H_2^+$ excluded further use of CH_3C_3N as a potential source of the C_3N^+ ion. Electron impact on dicyanoacetylene gave a satisfactory signal at m/z = 50 without contamination from other ions, and this was the preferred source for most of the reactions reported in this study. A mixture of C_4N_2 in helium was usually used to help reduce irregular emission currents caused by polymerization on the filament.

An examination of the reactivity of the C_3N^+ ion generated from C_4N_2, with H_2 and CH_4, revealed that the C_3N^+ ion existed almost exclusively (>95%) in the more reactive form. Rate coefficients and product distributions for this form of the ion were determined using C_3N^+ generated from C_4N_2. Rate coefficients for the less reactive form were determined using C_3N^+ generated from HC_3N. Product ratios could not be determined unambiguously for this form of C_3N^+ because of the presence of an excess

(8) The designation, C_3N^+, is used to represent the mixture of all isomers at m/z = 50 without regard to structure.

(9) Knight, J. S. Ph.D. Thesis, University of Canterbury, Christchurch, New Zealand, 1986.

(10) Knight, J. S.; Freeman, C. G.; McEwan, M. J. *J. Am. Chem. Soc.* **1986**, *108*, 1404.

(11) Knight, J. S.; Petrie, S. A. H.; Freeman, C. G.; McEwan, M. J.; McLean, A. D.; DeFrees, D. J. *J. Am. Chem. Soc.* **1988**, *110*, 5286.

(12) Petrie, S.; Freeman, C. G.; Meot-Ner, M.; McEwan, M. J.; Ferguson, E. E. *J. Am. Chem. Soc.* **1990**, *112*, 7121.

(13) Bohme, D. K.; Wlodek, S.; Raksit, A. B.; Schiff, H. I.; Mackay, G. I.; Keskinen, K. J. *Int. J. Mass Spectrom. Ion Processes* **1987**, *76*, 123.

(14) Bohme, D. K.; Wlodek, S.; Raksit, A. B. *Can. J. Chem.* **1987**, *65*, 1563.

(15) Parent, D. C. *Astrophys. J.* **1989**, *347*, 1183.

(16) Parent, D. C. *J. Am. Chem. Soc.* **1990**, *112*, 5966.

(17) Parent, D. C.; McElvany, S. W. *J. Am. Chem. Soc.* **1989**, *111*, 2393.

(18) Knight, J. S.; Freeman, C. G.; McEwan, M. J.; Adams, N. G.; Smith, D. *Int. J. Mass Spectrom. Ion Processes* **1985**, *67*, 317.

(19) Miller, F. A.; Mellon, D. H. *Spectrochim. Acta* **1967**, *23A*, 1415.

(20) Khanna, R. K.; Perera-Jarmer, M. A.; Ospina, M. J. *Spectrochim. Acta* **1987**, *43A*, 421.

(21) Durrant, M. C.; Kroto, H. W.; McNaughton, D.; Nixon, J. F. *J. Mol. Spectrosc.* **1985**, *109*, 8.

(22) Su, T.; Chesnavich, W. J. *J. Chem. Phys.* **1982**, *76*, 5183.

(23) Lias, S. G.; Bartmess, J. E.; Liebman, J. F.; Holmes, J. L.; Levin, R. D.; Mallard, W. G. *J. Phys. Chem. Ref. Data* **1988**, *17*, Supplement No. 1.

(24) Halpern, J. B.; Miller, G. E.; Okabe, H.; Nottingham, W. *J. Photochem. Photobiol., A* **1988**, *42*, 63.

Table I. Reaction Rate Coefficients and Product Distributions for Reactions of C_3N^+ with Various Neutral Reactants

reactant	products[a]	branching[a] ratio	k_1[b,c]	k_2[b,d]	k_c[b,e]	$-\Delta H_f°$[f] (kJ mol^{-1})
H_2	$HC_3N^+ + H$	0.90	0.81	<0.0005	1.50	158
	HC_3NH^+	0.10				721
CH_4	$C_2H_2N^+ + C_2H_2$	0.15				341
	(or $C_3H_4^+ + CN$)					212[g]
	$HC_3N^+ + CH_3$	0.50	0.97	<0.001	1.1	156
	$HC_3NH^+ + CH_2$	0.20				256
	$CH_3C_3N^+ + H$	0.15				180[h]
NH_3	$NH_3^+ + C_3N$	0.80	2.0	2.0	2.2	241[i]
	$CH_2N^+ + C_2HN$	0.20				
H_2O	$CH_2N^+ + C_2O$	0.05				[j]
	$HC_3N^+ + OH$	0.65	0.9	0.05	2.4	95
	$C_3NOH^+ + H$	0.30				>317
N_2	$C_3N{\cdot}N_2^+$		0.02	<0.0005	0.73	
O_2	$C_2N^+ + CO_2$	0.40	0.50	0.01	0.67	529[k]
	$C_3NO^+ + O$	0.60				>34[l]
CO	$C_3N{\cdot}CO^+$		0.54	<0.001	0.80	
C_2H_2	$HC_5N^+ + H$	0.95	1.0	>0.6[m]	1.0	
	$C_3N{\cdot}C_2H_2^+$	0.05				
HCN	$HC_3N^+ + CN$	0.98	2.2	0.23	3.3	76
	$C_3N{\cdot}HCN^+$	0.02				
CO_2	$C_3NO^+ + CO$		0.35	<0.001	0.79	[n]
C_2N_2	$NC4N^+ + CN$	0.20	1.2	0.07	1.0	49[o]
	$C_3N{\cdot}C_2N_2^+$	0.80				

[a] Products shown are those determined for the more abundant $CCCN^+$ isomer. Where more than one product channel was observed, the branching ratio determined is shown. [b] Rate coefficients are expressed in units of 10^{-9} cm^3 s^{-1}. [c] Rate coefficient of the more reactive $CCCN^+$ isomer determined using C_4N_2 as the source gas. [d] Rate coefficient for the less reactive c-C_3N^+ isomer determined using HC_3N as the source gas. [e] Collision rate coefficient calculated using the variational transition state theory of ref 22. [f] Calculated using $\Delta H_f°(CCCN^+)$ = 1850 kJ mol^{-1} as in refs 6 and 7 and using the thermodynamic data of ref 23. [g] Calculated assuming a $CH_2{=}C{=}CH_2^+$ structure for $C_3H_4^+$. [h] Calculated assuming $\Delta H_f°(CH_3C_3N^+)$ = 1378 kJ mol^{-1} as estimated in ref 23. [i] $\Delta H_f°(CCCN)$ = 629 kJ mol^{-1} from ref 24. [j] The occurrence of this channel required $\Delta H_f°(C_2O) \leq 661$ kJ mol^{-1}. [k] Calculated assuming a CCN^+ structure for C_2N^+. [l] Calculated using $\Delta H_f°(C_3NO^+) < 1567$ kJ mol^{-1} from the reaction of $C_3N^+ + CO_2$ (see *m* below). [m] See text for discussion. [n] The occurrence of this channel requires $\Delta H_f°(C_3NO^+) < 1567$ kJ mol^{-1}. [o] Calculated assuming the dicyanoacetylene structure for NC_4N^+.

of the more reactive component. The ratio of the two components was insensitive to electron energy. When the two forms of the ion reacted at substantially different rates (about a factor of 2 or greater), significant curvature was seen in the semilogarithmic plots of intensity of the m/z = 50 signal versus neutral reactant flow (as in Figure 1). The rate coefficients for the two forms were found using double exponential fitting of the decay curve as described previously.[10] The rate coefficients for both forms of C_3N^+ and product distributions for the more reactive form, with a range of neutral reactants, are summarized in Table I.

Evidence for Isomerism

The distinction on the basis of reactivity, between different forms of ions having the same general formula, does not necessarily imply the existence of structural isomers. Metastable electronic or vibrational excitation of a significant fraction of the reactant ions can also account for differences in reactivity. However, although most examples of long-lived vibrationally excited or metastable gas-phase cations are associated with diatomic ions, there is also some evidence to suggest that larger long-lived ions such as vibrationally excited C_4^+ can survive in a flow tube.[25] N_2 is often used as a quenching gas in flow tube experiments to remove excitation, as it is not chemically reactive with many ions. In the present case we observed N_2 to associate with the *more reactive* of the two forms of C_3N^+ but not with the less reactive component of the C_3N^+ ion swarm.

$$C_3N^+ + N_2 + M \rightarrow C_3N^+{\cdot}N_2 + M \qquad (1)$$

Such an association reaction is strongly indicative that the differences in reactivity between the two forms of C_3N^+ are *not* due to metastable excitation of the ions but arise because of differences in structure. The more abundant (~90%), more reactive component is much less likely to associate with N_2 than the less reactive second component, if excess internal energy is the source of the additional reactivity. Adduct formation requires the complex to survive long enough for collisional stabilization to occur: the presence of the additional excitation energy shortens the lifetime of the complex and would hinder association, not enhance it as we observed. Further, the less reactive (~10%) component of the C_3N^+ signal cannot be a more excited form of the major component, as the additional energy should also promote its reactivity. Only in the reactions with NH_3 and C_2H_2 did we observe the ~10% component of C_3N^+ to react at a rate greater than 10% of the collision rate.

We therefore conclude that two isomers of C_3N^+ are produced by electron impact on cyanoacetylene.

Isomer Identification

The more reactive and more abundant C_3N^+ component generated from HC_3N (~90%) and NCCCN (≥95%) was assigned the $CCCN^+$ structure after consideration of the parent neutral structure and the results of ab initio calculations which show this isomer to have the lowest energy.[7] We note that previous experience with cations of nitriles also supports the conclusion that the structure of the parent molecule influences the structure of the cation formed,[10] even when other lower energy isomers are possible.[12] But having made this assignment, we have now to reconcile the fact that the ~10% component of C_3N^+, which is less reactive than $CCCN^+$, is due to a higher energy isomer. In most systems of simple isomeric cations, the higher energy isomer is more reactive than the lower energy isomer (e.g., HCN^+ is more reactive than HNC^+;[12] CCN^+ is more reactive than CNC^+[11,13]), but not exclusively so. Other factors such as the height of the barrier on the energy surface can influence the outcome of a reaction, if rearrangement of an ion is required before reaction occurs, as was noted for the reactions of $NNOH^+$ and $HNNO^+$ with NO.[26]

(25) Giles, K.; Adams, N. G.; Smith, D. *Int. J. Mass Spectrom. Ion Processes* **1989**, *89*, 303.

The ab initio calculations provide two likely candidates for the identity of the less reactive, higher energy isomer: $CCNC^+$ and c-C_3N^+.[7] Of these, the isomer that best fits our experimental observations is the four-membered ring structure

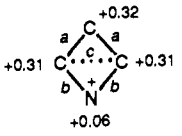

which we designate c-C_3N^+. This choice is consistent with the results of a near-monochromatic electron impact study of HC_3N which identified c-C_3N^+ as the second isomer, from the energy at which a break occurred in the ionization efficiency curve.[6] It is also consistent with the known reactivity of small cyclic isomers as compared with their acyclic counterparts. Studies of the isomers c-$C_3H_2^+$, HC_3H^+,[27,28] c-$C_3H_3^+$, and $CH_2C_2H^+$[29] all report a lower reactivity for the cyclic isomer. The c-C_3N^+ structure has calculated bond lengths that are similar to those expected in an aromatic heterocycle (a = 1.386 Å, b = 1.350 Å, and c = 1.542 Å),[7,36] it has a delocalized charge (shown in units of e) and is not expected to exhibit significant carbene activity.

Isomeric Ratio

We examined the reactivity of C_3N^+ from a number of different sources including electron impact (as described above) as well as several ion–molecule reactions in which C_3N^+ is produced. We felt that, by studying the reactivity of the C_3N^+ product of these ion–molecule reactions, we would obtain an alternative assessment of the relative heats of formation of the more reactive and less reactive isomers. Electron impact on HC_3N and NC_4N favors the formation of $CCCN^+$ by virtue of the source gas structure. The production of C_3N^+ in ion–molecule reactions in which the $CCCN^+$ structural fragment does not already exist within the reactants should give predominantly the isomers having the lowest heat of formation. Those reactions previously reported to produce C_3N^+ are (with the product channel efficiency shown in parenthesis) as follows:[18,30-34]

$$He^+ + HC_3N \longrightarrow C_3N^+ + H + He \quad (0.31) \qquad (2)$$
$$\Delta H_2 = -655 \text{ kJ mol}^{-1}$$

$$CN^+ + C_2N_2 \longrightarrow C_3N^+ + N_2 \quad (0.10) \qquad (3)$$
$$\Delta H_3 = -251 \text{ kJ mol}^{-1}$$

$$C_2^+ + C_2N_2 \longrightarrow C_3N^+ + CN \quad (0.30) \qquad (4)$$
$$\Delta H_4 = -20 \text{ kJ mol}^{-1}$$

$$C_2^+ + HCN \longrightarrow C_3N^+ + H \quad (1.0) \qquad (5)$$
$$\Delta H_5 = -65 \text{ kJ mol}^{-1}$$

$$C_2^+ + HC_3N \longrightarrow C_3N^+ + C_2H \quad (0.50) \qquad (6)$$
$$\Delta H_6 = +65 \text{ kJ mol}^{-1}$$

We exclude reaction 6 from this list because although C_3N^+ was reported as the major product of reaction in one study,[32,33] the other investigation of this reaction did not list C_3N^+ as a product.[18] We note also that production of C_3N^+ is 65 kJ mol^{-1} endothermic in reaction 6 given the experimental determination of $\Delta H_f°$($CCCN^+$) = 1850 kJ mol^{-1}.[6,7]

Table II. Isomeric Composition of C_3N^+ Ion Signal Produced by Different Methods

method of production	site of production[a]	percentage $CCCN^+$
e + HC_3N[b]	IS	90 ± 2[c]
e + He/HC_3N[b,d]	IS	90 ± 2[c]
e + C_4N_2[b]	IS	>95[c]
$C_2^+ + C_2N_2$	FT	>98[e]
$CN^+ + C_2N_2$	FT	>95[e]
$C_2^+ + HCN$	FT	>90[e]

[a] IS = ion source; FT = flow tube. [b] Electron impact of 30-eV electrons on stated gas. [c] Determined by the extent of reaction with H_2. [d] Using a 20/1 mixture of He/HC_3N. [e] Determined by reaction with N_2.

The C_3N^+ product in reactions 3, 4, and 5 was produced at the first inlet port by the addition of the appropriate reactant neutral (C_2N_2/HCN) at a sufficient flow rate so as to optimize the C_3N^+ signal. N_2, added at the second inlet port, was chosen as the diagnostic gas for determining the isomeric distribution as we have demonstrated that it associated with $CCCN^+$ only and did not react with other ion products of reactions 3–5. The extent of depletion of the C_3N^+ signal upon addition of N_2 then allowed a lower limit to the ratio $CCCN^+$/c-C_3N^+ to be obtained. The results for these reactions are summarized in Table II.

It is evident from the ratios shown in Table II that the more reactive isomer, $CCCN^+$, is consistently the predominant form of C_3N^+. Furthermore, the available heats of formation indicate that reactions 4 and 5 can produce only the lower energy isomer, $CCCN^+$, which supports our proposal that the more reactive isomer is indeed $CCCN^+$.

Reaction Chemistry of $CCCN^+$ and c-C_3N^+

The results in Table I reveal a contrast in reactivity of the two forms of C_3N^+: $CCCN^+$ reacts at close to the collision rate with most of the neutral reactants studied, whereas c-C_3N^+ is generally unreactive. Clearly, substantial barriers exist in the reactions of c-C_3N^+, possibly associated with ring opening. We were not able to find a source of C_3N^+ that gave c-C_3N^+ as the major isomer, and consequently we could not provide an unambiguous identification of the products of reaction of c-C_3N^+. In the discussion that follows, the products shown are the products of the $CCCN^+$ isomer.

H_2 and CH_4. H-atom abstraction (reactions 7a and 8b) is the major product channel in each reaction, but in the reaction with H_2 it occurs at a rate significantly below the collision rate. Several

$$CCCN^+ + H_2 \longrightarrow HC_3N^+ + H \quad (0.90) \qquad (7a)$$
$$\longrightarrow HC_3NH^+ \quad (0.10) \qquad (7b)$$

$$CCCN^+ + CH_4 \longrightarrow C_2H_2N^+ + C_2H_2 \quad (0.15) \qquad (8a)$$
$$(\text{or } C_3H_4^+ + CN)$$
$$\longrightarrow HC_3N^+ + CH_3 \quad (0.50) \qquad (8b)$$
$$\longrightarrow HC_3NH^+ + CH_2 \quad (0.20) \qquad (8c)$$
$$\longrightarrow CH_3C_3N^+ + H \quad (0.15) \qquad (8d)$$

authors have commented recently[28,35] that exothermic H-atom abstraction is often hindered by the existence of energy barriers when the neutral reactant is H_2. In the present case, the observation of a competing channel, which requires collisional stabilization of the complex, is consistent with the existence of a barrier to H-atom extraction. The products shown for reactions 7a and 7b, HC_3N^+ and HC_3NH^+, have been designated the assigned structures on the basis of energetics and subsequent reactivity with H_2.

In reaction 8a with CH_4, there are two possible exothermic channels giving rise to the 15% product ion at m/z = 40: the most exothermic channel leads to H_2CCN^+ (or H_2CNC^+) + C_2H_2 and the less exothermic channel to $C_3H_4^+$ + CN.

(26) Ferguson, E. E. *Chem. Phys. Lett.* **1989**, *156*, 319.
(27) Smith, D.; Adams, N. G. *Int. J. Mass Spectrom. Ion Processes* **1987**, *76*, 307.
(28) Prodnuk, S. D.; De Puy, C. H.; Bierbaum, V. M. *Int. J. Mass Spectrom. Ion Processes* **1990**, *100*, 693.
(29) Smyth, K. C.; Lias, S. G.; Ausloos, P. *Combust. Sci. Technol.* **1982**, *28*, 147.
(30) Mackay, G. I.; Vlachos, G. D.; Bohme, D. K.; Schiff, H. I. *Int. J. Mass Spectrom. Ion Processes* **1980**, *36*, 259.
(31) Schiff, H. I.; Bohme, D. K. *Astrophys. J.* **1980**, *232*, 740.
(32) Bohme, D. K.; Raksit, A. B. *Mon. Not. R. Astron. Soc.* **1985**, *213*, 717.
(33) Raksit, A. B.; Bohme, D. K. *Can. J. Chem.* **1985**, *63*, 854.
(34) Raksit, A. B.; Bohme, D. K. *Int. J. Mass Spectrom. Ion Processes* **1985**, *63*, 217.
(35) Adams, N. G.; Smith, D. *Int. J. Mass Spectrom. Ion Processes* **1984**, *61*, 133.
(36) Maclagan, R. G. A. R. Private communication.

Table III. A Comparison of $:C_nN^+$ (n = 2–7) Reactions with CH_4

reaction products	C_2N^+ [a,b]	C_3N^+ [c]	C_4N^+ [d]	C_4N^+ [e]	C_5N^+ [e]	C_7N^+ [e]
$CH_3^+ + HC_nN$				0.10	0.23[h]	0.23
$C_2H_3^+ + HC_{n-1}N$	0.60[h]		0.25[h]	0.18[h]	0.07	0.08
$C_{n-4}H_3^+ + HC_5N$					0.23[h]	0.10
$C_{n-2}H_3^+ + HC_3N$			0.25[h]	0.18[h]	0.07	
$C_nH_3^+ + HCN$	0.60[h]		0.30	0.34	0.07	
$H_2CN^+ + C_nH_2$	0.10[h]		0.05	0.11	0.08	0.08
$H_2C_{n-1}N^+ + C_2H_2$	0.10[h]	0.15	0.35	0.17	0.09	0.14
$HC_nN^+ + CH_3$		0.50		0.01	0.37	0.33
$H_2C_nN^+ + CH_2$		0.20				
$H_2C_{n+1}N^+ + H_2$	0.30		0.05	0.07	0.04	
$H_3C_{n+1}N^+ + H$		0.15				
rate coefficient (in units of 10^{-10} cm^3 s^{-1})	3.5[a,f] 7.0[b,f]	9.7[g]	5.7	7.0	7.5	4.6

[a] Reference 13. [b] Reference 11. [c] This work. [d] Reference 14. [e] Reference 16. [f] Rate coefficient for $:CCN^+$ isomer. [g] Rate coefficient for $:CCCN^+$ isomer. [h] Indicates the product channel is listed twice in two categories in this column.

Several studies in the literature are available for comparison with the present work of the reactions with CH_4. We have noted in the Introduction that the chemistry of the C_nN^+ cations has been interpreted in terms of their carbene character.[13-17] Semiempirical MNDO calculations[16] support the carbene designation, $:C_nN^+$, for the cation, in which most of the charge is found to reside on the terminal C atom and an alternation in bond length along the C chain is also predicted. Although the C_nN^+ structures reported appear to refer to a higher energy singlet state and not the lower energy triplet state, the structure of the two states does not change with multiplicity.[16] Ab initio calculations made at the 6-311G** level of theory for C_3N^+[7,36] depict an ion that does not have an alternation in bond length nor does it have the same accumulation of charge on the terminal C atom.

$$\overset{+0.43}{C}\overset{1.32}{=}\overset{+0.03}{C}\overset{1.29}{=}\overset{+0.43}{C}\overset{1.22}{=}\overset{+0.11}{N}$$

The bond length in Å and the charge in units of e are shown. If these calculations provide reasonable representations of the appropriate cations, then some minor differences in product distribution might be anticipated between the reactions of C_3N^+ and its larger homologues. The reactions of $:C_nN^+$ with CH_4, including the present results for $:C_3N^+$, are summarized in Table III from which it is evident that for all odd values of n, H-atom abstraction is the major channel. It is also apparent that there are some large differences between the product distributions of C_3N^+ in this study and the results for C_5N^+ and C_7N^+ in the FTICR study of the larger homologues.[16] The second most important channel for C_5N^+ and C_7N^+ was the channel leading to $CH_3^+ + HC_nN$, which was not found for C_3N^+ in spite of being more exothermic ($\Delta H°$ = −330 kJ mol^{-1}) than the observed H-atom abstraction channel ($\Delta H°$ = −156 kJ mol^{-1}). Differences in product distribution to this extent may simply reflect the specific nature of each potential energy surface, or they may indicate a difference of a more fundamental nature such as different isomers of C_nN^+ being present. In the FTICR study, the C_nN^+ ions were generated in the reactions

$$C_{n-1}^+ + HCN \rightarrow C_nN^+ + H \qquad (9)$$

where the C_{n-1}^+ precursor ions were formed from laser ablation of graphite. It is not clear, however, whether the C_nN^+ ion products of reaction 9 have a linear structure with a terminal N atom or some other structure. We note that the analogous reaction of $C^+ + HCN$ is known to form the CNC^+ isomer only from ground-state C^+ although for n = 2, the CNC^+ isomer is more stable than the CCN^+ form.[11]

The C_nN^+ ions (n = 2–4) in the three SIFT investigations have all been generated by electron impact on the appropriate neutral: C_2N^+ from C_2N_2,[11,13] C_4N^+ from H_2CCHCH_2CN,[14] and C_3N^+ in the present case from HC_3N or NCCCN. In two of these studies, the isomeric form of the C_nN^+ was identified: in the third study, for C_4N^+, it was assumed that the most likely structure for C_4N^+ was $:CCCCN^+$.[14] A comparison of the reaction chemistry of these ions with selected neutral reagents is given in Table IV.

NH_3. The reaction with ammonia was the only reaction studied for which both isomers showed the same reactivity. The major product channel for the reaction of each isomer was charge transfer which is very exothermic for $CCCN^+$ and presumably also for c-C_3N^+ although we are not aware of any determination of $\Delta H_f°$(c-C_3N). The second 20% channel leading to $CH_2N^+ + C_2HN$ is likely to be quite exothermic as well.[37]

H_2O and HCN. Again H-atom abstraction is the major channel observed for these reactions, although the relatively low rate coefficient for reaction 10b is surprising as this type of process usually occurs at close to the collision rate for reactants other than H_2. The occurrence of reaction 10c leading to the C_3NOH^+ ion

$$CCCN^+ + H_2O \longrightarrow CH_2N^+ + C_2O \quad (0.05) \quad (10a)$$
$$\longrightarrow HC_3N^+ + OH \quad (0.65) \quad (10b)$$
$$\longrightarrow C_3NOH^+ + H \quad (0.30) \quad (10c)$$

$$CCCN^+ + HCN \longrightarrow HC_3N^+ + CN \quad (0.98) \quad (11a)$$
$$\longrightarrow C_3N^+ \cdot HCN \quad (0.02) \quad (11b)$$

implies that $\Delta H_f°(C_3NOH^+) \leq 1390$ kJ mol^{-1}, which is consistent with what is known of the thermochemistry of the NCCH=C=O$^+$ ion.[23] The reaction of C_3N^+ with HCN may be compared to an FTICR study of $:C_nN^+$ (n = 4–10) with HCN in which the results for C_5N^+ and C_7N^+ are as follows:[17]

$$C_nN^+ + HCN \longrightarrow HC_nN^+ + CN \qquad (12a)$$
$$\longrightarrow NC_{n+1}N^+ + H \qquad (12b)$$
$$\longrightarrow \text{adduct} \qquad (12c)$$

In the present case, almost all reactive collisions resulted in H-atom abstraction, and channel 12b (57% for C_5N^+, 21% for C_7N^+) leading to CN addition was absent even though it is more exothermic for C_3N^+ ($\Delta H°$ = −94 kJ mol^{-1}) than is channel 12a ($\Delta H°$ = −76 kJ mol^{-1}). Again these results support the conclusion reached in the reactions with CH_4, that different isomeric forms of C_nN^+ are present in the two studies.

CO and N_2. Association leading to the stabilized adduct was the only channel observed for these reactants. In each instance, the rate of adduct formation is surprisingly large. For the reaction with CO, about 67% of all collisions lead to the stabilized complex.

$$CCCN^+ + CO \rightarrow C_3N \cdot CO^+ \qquad (13)$$

$$k = 5.4 \times 10^{-10} \text{ cm}^3 \text{ s}^{-1}$$

Such an outcome implies an appreciable potential well on the $C_3N \cdot CO^+$ energy surface leading to the stabilized adduct, as the excited complex must survive sufficiently long for stabilization

(37) Hirano, T.; Nakagawa, N.; Murakami, A.; Nomura, O. *Chem. Phys. Lett.* **1989**, *162*, 89.

Table IV. A Comparison of $:C_nN^+$ (n = 2–4) Reaction Products and Rate Coefficients with the Designated Reactant

	$:C_2N^{+\,a,b,c}$			$:C_3N^{+\,d}$			$:C_4N^{+\,e}$		
reactant	branching fraction	reaction products	rate coeff[f]	branching fraction	reaction products	rate coeff[f]	branching fraction	reaction products	rate coeff[f]
H_2	[0.9] [0.1]	$CH_2N^+ + C$ $C_2H_2N^+$	(0.9)[a] (0.3)[b]	[0.9] [0.1]	$HC_3N^+ + H$ HC_3NH^+	(0.81)	[1.0]	$C_3H^+ + CHN$	(0.022)
CH_4	[0.65] [0.15] [0.20]	$C_2H_3^+ + CHN$[g] $H_2CN^+ + C_2H_2$[g] $H_2C_3N^+ + H_2$[h]	(0.70)[a] (0.35)[b]	[0.15] [0.50] [0.20] [0.15]	$C_2H_2N^+ + C_2H_2$ $HC_3N^+ + CH_3$ $HC_3NH^+ + CH_2$ $CH_3C_3N^+ + H$	(0.97)	[0.05] [0.25] [0.35] [0.30] [0.05]	$CH_2N^+ + C_4H_2$ $C_2H_3^+ + C_3HN$ $C_3H_2N^+ + C_2H_2$ $C_4H_3^+ + CHN$ $C_5H_2N^+ + H_2$	(0.57)
NH_3	[1.0]	$H_2CN^+ + HCN$	(1.9)[a] (1.8)[b]	[0.80] [0.20]	$NH_3^+ + C_3N$ $CH_2N^+ + C_2HN$	(2.0)	[0.65] [0.15] [0.20]	$NH_3^+ + C_4N$ $CH_2N^+ + C_3HN$ $C_3H_2N^+ + CHN$	(1.2)
H_2O	[0.5] [0.3] [0.2]	$CHO^+ + CHN$ $C_2NO^+ + H_2$ $CH_2N^+ + CO$	(1.6)[a] (1.0)[b]	[0.05] [0.65] [0.30]	$CH_2N^+ + C_2O$ $HC_3N^+ + OH$ $C_3NOH^+ + H$	(0.9)	[0.40] [0.50] [0.10]	$CHO^+ + C_3HN$ $C_3H_2N^+ + CO$ $C_4H_2NO^+$	(1.5)
C_2H_2	[0.20] [0.80]	$CH_2N^+ + C_3$ $C_3H^+ + CHN$	(1.6)[a] (1.0)[b]	[0.95] [0.05]	$HC_5N^+ + H$ $C_3N{\cdot}C_2H_2^+$	(1.0)	[≥0.7] [≤0.3]	$C_5H^+ + CHN$ $C_6H_2N^+$	(0.80)
HCN	[1.0]	$C_3HN_2^+$	(0.42)[a] (0.29)[b]	[0.98] [0.02]	$HC_3N^+ + CN$ $C_3N{\cdot}HCN^+$	(2.2)	[1.0]	$C_5HN_2^+$	(0.84)
CO	[1.0]	C_3NO^+	(≤0.0005)	[1.0]	$C_3N{\cdot}CO^+$	(0.54)	[1.0]	C_5NO^+	(0.093)
O_2	[1.0]	$C_2NO^+ + O$	(0.35)	[0.40] [0.60]	$C_2N^+ + CO_2$ $C_3NO^+ + O$	(0.50)			

[a] From ref 13. [b] From ref 14. [c] The products and rate coefficients shown are for the $:CCN^+$ isomer unless indicated otherwise. [d] This work. [e] From ref 14. The $:C_4N^+$ ion was not characterized but may have the $:CCCCN^+$ structure. [f] Rate coefficient for total loss of $:C_nH^+$ ion in units of 10^{-9} cm^3 s^{-1}. [g] The products shown are for a mixture of isomers in the ratio $CCN^+/CNC^+ \sim 0.25$.

to occur by collision with the helium bath gas. A comparison with the CO reactions of C_2N^+ and C_4N^+ in Table IV shows that the association adduct of CO is formed for all ions, but for C_3N^+, the rate coefficient is very much larger. A possible product of reaction 13 is $O{=}C{=}C{=}C{=}C{=}N^+$ which is resonance stabilized.

Only 3% of C_3N^+/N_2 collisions result in the formation of a stabilized adduct, but this in itself is unusual as N_2 complexes usually have shallow wells in the energy surface, which result in lower association rates. The product ion in this case,

$$CCCN^+ + N_2 \rightarrow C_3N_3^+ \qquad (14)$$

$C_3N_3^+$, has also been reported as a product of the reaction of $C_4N_4^+$ with C_2N_2.[34] The same number of internal modes are available in $C_3N_3^+$ as in the CO adduct of C_3N^+, amongst which the energy can be distributed. The much lower efficiency of stabilization in this case is indicative of a shallower well for the $C_3N_3^+$ adduct, and the identity of the $C_3N_3^+$ species is not known. The complex is possibly electrostatic in nature, in view of the shallow potential well, although a strained covalent structure of the form

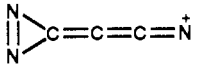

could be envisaged which would result from carbene addition to the N_2 bond.

C_2H_2. In the collision-rate reaction with C_2H_2, adduct formation followed by H loss led to the main ion product observed, with the C_5NH^+ ion probably having the cyanodiacetylene structure, HC_5N^+.

$$CCCN^+ + C_2H_2 \longrightarrow C_5NH^+ + H \quad (0.95) \qquad (15a)$$

$$\longrightarrow C_3N{\cdot}C_2H_2^+ \quad (0.05) \qquad (15b)$$

The occurrence of this channel is consistent with what is known of the thermochemistry of HC_5N^+.[38] We could establish only a lower limit for the rate coefficient for the reaction of c-C_3N^+ with C_2H_2 because small amounts of HC_3N^+ (injected as an impurity ion with C_3N^+) also reacted with C_2H_2, producing a product ion, coincident in mass with the C_3N^+ reactant ion.[39]

$$HC_3N^+ + C_2H_2 \longrightarrow C_4H_2^+ + HCN \quad (0.60) \qquad (16a)$$

$$\longrightarrow C_2H_2^+ + HC_3N \quad (0.05) \qquad (16b)$$

$$\longrightarrow HC_3N^+{\cdot}C_2H_2 \quad (0.35) \qquad (16c)$$

Although the limit established for the reaction rate coefficient of c-C_3N^+ with C_2H_2 was $k > 6 \times 10^{-10}$ cm^3 s^{-1}, the reaction is undoubtedly faster than this and probably occurs at close to the collision rate. Comparison of the reactions of C_nN^+ with C_2H_2 in Table IV shows that a prominent channel for even values of n is the reaction

$$:C_nN^+ + C_2H_2 \rightarrow HC_{n+1}^+ + HCN \qquad (17)$$

but this channel was not observed for n = 3, in keeping with the expected higher enthalpies of formation of the $C_{n+1}H^+$ ions when n is odd compared to the values for even n.[40]

O_2 and CO_2. O-atom abstraction was the major channel observed in these reactions. Assuming that reactions 18b and 19 provide exothermic pathways to the ion C_3NO^+, then $\Delta H_f^\circ(C_3NO^+) < 1567$ kJ mol^{-1}. The structure of this ion is not known, but we anticipate a reaction at the carbene end of $:CCCN^+$ leading to $O{=}C{=}C^+{-}C{=}N$. Reaction at this site also accounts for the production of C_2N^+ in reaction 18a (most probably as the higher energy CCN^+ isomer)[11] through carbene insertion into the O_2 bond followed by CO_2 loss.

$$CCCN^+ + O_2 \longrightarrow C_2N^+ + CO_2 \quad (0.40) \qquad (18a)$$

$$\longrightarrow OC_3N^+ + O \quad (0.60) \qquad (18b)$$

$$CCCN^+ + CO_2 \longrightarrow OC_3N^+ + CO \quad (1.0) \qquad (19)$$

C_2N_2. The reaction between C_3N^+ and C_2N_2 has been reported previously but without regard to the isomeric form of C_3N^+.[34] The product ratio reported in the earlier study is in good agreement with this work, but we find the reaction to occur at the collision rate ($k_{CCCN^+} = 1.2 \times 10^{-9}$ cm^3 s^{-1}) for the $CCCN^+$ isomer, which

(38) Sen, A. D.; Huntress, W. T.; Anicich, V. G.; McEwan, M. J.; Denison, A. B. *J. Chem. Phys.* **1991**, *94*, 5462.

(39) Petrie, S.; Freeman, C. G.; McEwan, M. J. *Mon. Not. R. Astron. Soc.* **1992**, *257*, 438.

(40) McElvany, S. W.; Dunlap, B. I.; O'Keefe, A. *J. Chem. Phys.* **1987**, *86*, 715.

is much larger than the value reported previously of $k = 4.5 \times 10^{-10}$.

$$CCCN^+ + C_2N_2 \longrightarrow C_4N_2^+ + CN \quad (0.20) \quad (20a)$$
$$\longrightarrow C_3N^+ \cdot C_2N_2 \quad (0.80) \quad (20b)$$

Conclusion

Electron impact of HC_3N generates two isomers of C_3N^+. The more abundant form is $CCCN^+$, and it is considered that the less abundant isomer is more likely to be c-C_3N^+ than $CCNC^+$. A notable finding of this work was that the lower energy isomer, $CCCN^+$, was found to be more reactive than the higher energy isomer designated c-C_3N^+.

The different reactivities of the two isomers can be rationalized in terms of the structures proposed for each isomer. $CCCN^+$, because of its carbene character, might be anticipated to be reactive. Carbene attack on the neutral reagent, followed by some rearrangement, can explain the formation of many products. c-C_3N^+, on the other hand, exhibits activation barriers in most of its reactions which are probably linked with ring opening requirements. The much lower reactivity of the cyclic isomer is also consistent with the lower reactivity observed for the cyclic isomers of the hydrocarbon ions such as $C_3H_2^+$ and $C_3H_3^+$.

Acknowledgment. We thank Dr. Alan Happer for helpful discussions, Mr. Barry Wells for the preparation of CH_3C_3N, and Mr. Paul Wilson for assistance with some of the measurements reported here. We also thank one of the referees for their comments leading to the inclusion of Tables III and IV.

The S_N2 Identity Exchange Reaction $ClCH_2CN + Cl^- \rightarrow Cl^- + ClCH_2CN$: Experiment and Theory

Brian D. Wladkowski, Kieran F. Lim,[†,1] Wesley D. Allen,* and John I. Brauman*

Contribution from the Department of Chemistry, Stanford University, Stanford, California 94305-5080, and Department of Chemistry, University of New England, Armidale NSW 2351, Australia. *Received January 22, 1992. Revised Manuscript Received April 29, 1992*

Abstract: The rate of substitution for the title reaction has been measured in the gas phase using Fourier transform ion cyclotron resonance (FT-ICR) spectrometry. The value of the observed rate coefficient is found to be $3.3 \pm 1.0 \times 10^{-10}$ cm^3 s^{-1} at 350 K, a reaction rate approximately one-tenth of the electrostatic ion–molecule collision rate. The experimental complexation energy for the formation of the intermediate ion–molecule complex, $[ClCH_2CN \cdot Cl]^-$, has also been measured using FT-ICR spectrometry by bracketing the associated equilibrium constant relative to values for compounds with known chloride affinities. Hence, $\Delta H^\circ_{350} = -19.4$ kcal mol^{-1} is obtained for the enthalpy of complexation at 350 K. By applying RRKM theory with the microcanonical variational transition state (μVTS) criterion to model the reaction, it is deduced that the observed experimental efficiency corresponds to an S_N2 transition state 5.9 kcal mol^{-1} *below* the separated reactants, or 13.5 kcal mol^{-1} above the intermediate ion–molecule complex. To further elucidate the potential surface for the title reaction and to provide data for the RRKM analysis, high-level ab initio quantum chemical results have been determined. In particular, the geometric structures, relative energies, and vibrational frequencies of four salient stationary points on the potential surface (separated reactants, two ion–dipole complex structures, and the S_N2 transition state) have been investigated at various levels of theory ranging from 3-21G RHF to 6-31+G(d,p) MP4 to TZ3P+(2f,d)+diffuse MP2. The ab initio results predict the ion–dipole complex and the S_N2 transition state to lie 18.4 and 6.9 kcal mol^{-1}, respectively, below the separated reactants, in excellent agreement with experiment. For comparison, improved theoretical predictions are obtained for the CH_3Cl/Cl^- system, viz. a complexation energy of 10.6 kcal mol^{-1} and an S_N2 barrier 1.8 kcal mol^{-1} *above* the separated reactants. Qualitative bonding models describing the effect of α substitution on the stability of S_N2 transition states are subsequently analyzed using the ab initio results for the CH_3Cl/Cl^- and $ClCH_2CN/Cl^-$ systems. The α effect in these systems appears not to arise from "resonance" effects in the transition state.

I. Introduction

Detailed experimental studies in the early 1950s established the fundamental mechanism for bimolecular nucleophilic substitution (S_N2) reactions in solution and laid the groundwork for much of what is known today about this pervasive chemical process.[2,3] Since the early 1970s, much work has focused on the characteristics of these reactions in the gas phase in order to more clearly understand both "intrinsic" and solvent effects.[4-14] In the study of intrinsic features of S_N2 processes, identity exchange reactions, in which the entering and leaving groups are the same, are especially useful. However, S_N2 identity exchange in the gas phase is often too slow to be measured because of large activation barriers. Nevertheless, gas-phase investigations of such processes have recently become experimentally realizable through the discovery of sufficiently fast reactions, and a few examples of chloride- and bromide-ion exchange have been documented.[15-17]

The α-substitution effect and the applicability of Marcus theory[18] to S_N2 systems are two issues for which a more complete

[†] Department of Chemistry, University of New England.

(1) Archbishop Mannix Traveling Scholar, 1988-1990.
(2) Streitwieser, A. *Solvolytic Displacement Reactions*; McGraw-Hill: New York, 1962.
(3) Lowry, T. H.; Richardson, K. S. *Mechanism and Theory in Organic Chemistry*, 3rd ed.; Harper and Row: New York, 1987.
(4) Brauman, J. I.; Olmstead, W. N.; Lieder, C. A. *J. Am. Chem. Soc.* **1974**, *96*, 4030.
(5) Olmstead, W. N.; Brauman, J. I. *J. Am. Chem. Soc.* **1977**, *99*, 4219.
(6) Pellerite, M. J.; Brauman, J. I. *J. Am. Chem. Soc.* **1980**, *102*, 5993.
(7) Pellerite, M. J.; Brauman, J. I. *J. Am. Chem. Soc.* **1983**, *105*, 2672.
(8) Dodd, J. A.; Brauman, J. I. *J. Am. Chem. Soc.* **1984**, *106*, 5356.
(9) Dodd, J. A.; Brauman, J. I. *J. Phys. Chem.* **1986**, *90*, 3559.
(10) Han, C.-C.; Dodd, J. A.; Brauman, J. I. *J. Phys. Chem.* **1986**, *90*, 471.
(11) Brauman, J. I.; Dodd, J. A.; Han, C.-C. *Adv. Chem. Ser.* **1987**, *No. 215*, Chapter 2.
(12) Caldwell, G.; Magnera, T. F.; Kebarle, P. *J. Am. Chem. Soc.* **1984**, *106*, 959.
(13) Tanaka, K.; Mackay, G. I.; Payzant, J. D.; Bohme, D. K. *Can. J. Chem.* **1976**, *54*, 1643.

0002-7863/92/1514-9136$03.00/0